Sensors & Diagnostics

CRITICAL REVIEW

View Article Online
View Journal | View Issue

Cite this: *Sens. Diagn.*, 2024, **3**, 1428

Antibody conjugates as CT/MRI Theranostics for diagnosis of cancers: a review of recent trends and advances

Saba Abaei,[ab] Ali Tarighatnia,[c] Asghar Mesbahi[d] and Ayuob Aghanejad *[ae]

The constant need for cancer diagnosis in the early stages drives the development of contrast agents and imaging methods. Imaging agents have important roles in monitoring the progression and metastasis of cancers. Antibodies as biomolecules in conjugation with nanoparticles, radioisotopes, and drugs have been used as biomarkers for the early diagnosis/therapy of cancers due to their serum stability, affinity, and specificity. While antibodies are commonly used as nuclear medicine biomarkers, antibody-based contrast agent platforms have recently gained attention in X-ray computed tomography (CT) and magnetic resonance imaging (MRI). The developing antibody-based contrast agents have revolutionized cancer imaging techniques, particularly through MRI. Despite the promising advancements, some challenges and limitations need to be addressed for the extensive applications of these agents. Ongoing research is focused on overcoming challenges and limitations to enhance the efficiency and accuracy of these imaging methods. With continued advancements, antibody-based contrast agents hold immense potential in the early diagnosis and treatment of cancer. In this review, we summarize and categorize the recent progress in targeted imaging using antibody-based contrast agents by MRI and CT modalities.

Received 28th April 2024,
Accepted 12th August 2024

DOI: 10.1039/d4sd00132j

rsc.li/sensors

1. Introduction

Cancer is a significant global public health issue that burdens society, early diagnosis of cancer is crucial for prevention and effective management.[1] Conversely, delayed detection can lead to higher costs of cancer care and increased mortality rates.[2] Two commonly used imaging tools for cancer detection are CT and MRI. MRI is a technology that utilizes non-ionizing radiation to produce images by observing the signal of hydrogen nuclei in response to magnetic fields, employing various distinct sequences.[3] CT imaging, on the other hand, is a non-invasive technology that utilizes different levels of X-ray absorption to create cross-sectional and three-dimensional (3D) images. Despite the ability of these two diagnostic methods to detect cancer, commonly used contrast agents (CAs) are employed to improve the differentiation between tumor and normal tissues. These CAs are designed to enhance the contrast and its impact on the region of interest.[4] However, these routinely used contrast agents have certain drawbacks, such as poor biocompatibility, short circulation times, and ineffective targeting. These limitations are considered restrictions in clinical usage.[5,6] Fortunately, developing contrast agents using targeted nanoparticles (NPs) has provided new insights into overcoming these limitations.

Molecules or biomarkers linked to a particular disease or cancer can serve as targets in cancer therapy.[7–9] The NPs can be conjugated with specific antibodies that target proteins or biomarkers expressed on the surface of cancer cells. Active targeting enhances nanoparticle delivery through interactions between targeting agents (such as antibodies, peptides, and folic acids) and adjacent biomarkers on cancer cells. These conjugates have been applied in diagnostic or theranostic platforms, each presenting unique advantages and disadvantages, as outlined in Table 1. Among them, antibody-nanoconjugates (Ab-NPCs) offer numerous advantages, such as the precise delivery of targeted molecules, chemical protection, and decreased toxicity. Antibodies can be designed or selected to specifically recognize and bind to this target molecule. Abs have been used as molecular imaging agents through a process called antibody-based molecular imaging.[10]

Antibodies are effective as theranostics agents due to their high affinity to bind specifically to a target molecule in tumor

[a] *Research Center for Pharmaceutical Nanotechnology, Biomedicine Institute, Tabriz University of Medical Sciences, Tabriz, Iran.*
E-mail: aghanejaday@tbzmed.ac.ir; Tel: +98 41 33367914
[b] *Department of Medical Physics, School of Medicine, Tabriz University of Medical Sciences, Tabriz, Iran*
[c] *Department of Medical Physics, School of Medicine, Ardabil University of Medical Sciences, Ardabil, Iran*
[d] *Radiation Oncology Department Olivia Newton-John Cancer, Wellness and Research Centre, Austin Health, Melbourne, Australia*
[e] *Department of Nuclear Medicine, Faculty of Medicine, Imam Reza General Hospital, Tabriz University of Medical Sciences, Tabriz, Iran*

Table 1 Advantages and disadvantages of different types of targeting agents

Targeting agents	Advantages	Disadvantages	Ref.
Antibodies	Improve the interaction of NPs with tumors Promote NPs accumulation in the tumor	Delivery challenges The cost, intricacy, and challenge of acquiring regulatory approval	11, 12
Peptides	Favorable biodistribution profiles Low molecular weight Fast clearance from the bloodstream Higher uptake in the target	Delivery challenges Maintaining the structural confirmation of peptides while attaching them to NP surfaces is challenging	13–15
Folic acids	Biocompatible Non-immunogenic Small molecule ligands with increased stability and a higher specific binding affinity Inexpensive	Delivery challenges Limited due to solubility issue Enlarge the conjugates' particle size Not all types of cancer show an overexpression of folic acid Peptidase-mediated digesting	16, 17

cells.[18,19] Different labeling techniques, such as radioisotope labeling for nuclear imaging, fluorophore labeling for optical imaging, and nanoparticles (NPs) labeling for X-ray computed tomography (CT) imaging and magnetic resonance imaging (MRI) have been used to produce antibody-conjugates for visualization and detection of molecular targets using appropriate imaging modalities to diagnose cancers and monitoring of treatment response.[20–22]

The delivery of NPs to tumors for therapeutic purposes and the use of nanoparticle-based contrast agents for tumor imaging both rely on the fact that nanoparticles primarily accumulate in solid tumor tissues after systemic injection.[23] Moreover, antibody-armed NPs offer several advantages over other delivery methods, as multiple ways exist to direct NPs to the desired area. Additionally, due to their small size, NPs can easily penetrate the rapidly growing tumor mass, accumulate in significant quantities at the site, and remain available within the tumor mass for an extended period.[24] Traditionally, researchers have sought to optimize NP-based CAs delivery through passive or active targeting techniques.[25] It should be noted that there might be variations in specific methodologies depending on factors like nanoparticle type, conjugation chemistry used, and targeted application; thus, detailed protocols should be consulted for each individual study design or application. This review emphasizes advances in the development of nanoparticle-based antibody conjugates (NPCs) and bioimaging applications as diagnostic or theranostic molecular probes in cancers. Moreover, we discussed the advantages and disadvantages of the imaging techniques, presented potential solutions, highlighted recent accomplishments, and addressed the current challenges in bioimaging applications of antibody nanoconjugates.

2. Nanoparticle-based antibody conjugates (NPCs) for CT and MR imaging

In CT imaging, nanoparticles can be loaded with a contrast agent, such as iodine, which enhances the visibility of tissues and organs during imaging. By conjugating antibodies to these nanoparticles, they can be directed towards a specific target in the body, such as cancer cells. This enables more accurate visualization and detection of tumors or diseased tissue.[26,27]

In MRI imaging, nanoparticles can be doped with paramagnetic ions that affect the relaxation times of water molecules around them. Antibody-conjugated nanoparticles can specifically bind to targeted biomarkers within tissues or cells, enabling enhanced contrast and improved visibility in MRI scans.[28]

The antibodies serve as a recognition element that guides the nanoparticles to the tumor site, improving their selective accumulation and retention in cancerous tissues.[29] Antibody conjugates can indeed be used as CT/MRI agents for diagnosis of cancers. These conjugates combine specific antibodies with contrast agents, allowing them to target and accumulate in cancer cells or tumor tissues.[30,31] In MRI, they can enhance the contrast between normal and diseased tissues, enabling better visualization of tumors.[32,33] Similarly, in CT scans, they can improve the visibility of tumors by increasing X-ray attenuation. Additionally, these antibody-conjugated NPs can be loaded with other diagnostic agents or therapeutic payloads for multifunctional applications like drug delivery or localized therapy.[29,34]

Therefore, antibody-conjugated nanoparticles are a promising approach to cancer detection. These nanoparticles are designed to specifically bind to cancer cells or tumor markers, enhancing the detection of cancer through various imaging techniques such as CT, MRI, or fluorescence imaging. Antibody nano-conjugates can still face delivery challenges, including accumulation in malignant tissue and movement through the tumor stroma. These obstacles can be overcome by improving the interaction between nanoparticles and tumors through targeting modalities.[13]

Overall, antibody-based molecular imaging offers a powerful tool for visualizing specific molecules *in vivo* and provides valuable information about disease processes at both cellular and molecular levels.[35] Antibody-conjugated nanoparticles can be used as CT and MRI imaging agents by attaching specific antibodies to the surface of nanoparticles. This targeting strategy allows for the detection and

visualization of specific biomarkers or targets in tissues or cells.[36,37] The following sections provide a detailed description of the structures of antibody-conjugated nanoparticles as targeted contrast agents, emphasizing the importance of the topic and the differences in the mechanisms and principles of CT and MRI imaging modalities.

3. Antibody-conjugated nanoparticles as MRI contrast agents

The alteration in the magnetization of hydrogen atoms within water, a crucial factor in determining the contrast capacity generated by the contrast agent, serves as the general mechanism of the contrast agent in MRI.[38] MRI contrast materials can be categorized into two types: T1, also referred to as positive contrast agents, which decrease longitudinal relaxation times and enhance the brightness of the accumulation area. Conversely, T2, or negative contrast agents, darken the immediate and surrounding region and decrease transversal relaxation times.

The contrast agents employed in MRI may have varying compositions, although many rely on utilizing highly paramagnetic ions such as Mn^{2+}, Fe^{3+}, and Gd^{3+}.[39] While developing contrast agents (CAs) has significant advantages, both T1 and T2 agents have their own drawbacks. Positive CAs are more toxic and have a shorter circulation time, while negative CAs can diminish the imaging signal. As a result, images may appear darker with lower signal, and high magnetic field inhomogeneities and sensitivity effects can introduce artifacts. Consequently, lesions are often confused with weak signals from surrounding normal tissues, leading to slightly lower sensitivity in pathological diagnosis.[40] Also, dual signal hybrid T1/T2 MRI contrast agents have emerged, offering enhanced relaxometry, low cytotoxicity, and improved image accuracy through self-confirmation, enabling better differentiation between normal and pathological regions.[41,42] Table 2 categorized the advantages and disadvantages of T1 and T2 based MRI contrast agents.

By utilizing antibody nanoconjugates as MRI imaging agents, it becomes possible to visualize and assess molecular targets associated with various diseases or conditions at a cellular level with improved sensitivity and specificity compared to traditional contrast agents alone.[54] These subsections cover three common substances in MRI contrast nanoparticles: gadolinium, manganese, and iron oxide. Each subsection outlines the contrast produced by each substances and the benefits of using antibody conjugates for detection or treatment.

3.1. Gadolinium-based antibody conjugates as T1 MRI contrast agents

Gadolinium-based contrast agents (GBCAs) are metallic substances with paramagnetic properties that generate a magnetic field to enhance the MRI signal. Since the 1980s,

Table 2 Classification of MRI contrast agents along with their advantages and disadvantages

Contrast type	Advantages	Disadvantages	Ref.
T1	Favorable for clinic Faster recovery High-permanent magnetic moment Improve the imaging sensitivity Smaller than usual molecules Quickly eliminated by the kidneys	Low signal intensity Induction NSF and brain lesions Require to receive large volume contrast administrations Short circulation time High toxicity Limitations on imaging versatility arise from negative photon interactions with the biological matrix, affecting energy transfer based on distance and altering signal intensity	43–49
T2	Biocompatibility Unique magnetic property Long blood half-lives Flexible surface chemistry High-saturation magnetization (Ms) values	Blooming effects Confuse tumors with hemorrhage or calcification signals Ineffective targeting Darkening of the image and poor resolution	40, 43, 46, 47, 50
T1/T2	Remove the challenge of image matching between various imaging instruments Specific lesion localization Ensuring imaging sensitivity Enhancing imaging accuracy Being able to validate reconstruction and data visualization in a more accurate and reliable manner Eliminating or reducing the limitations of MRI's weak sensitivity in detecting metastatic foci Image quantification of molecular targets and acquisition of T1 and T2 magnetic resonance signals in various tumors can be achieved using a novel two-way magnetic resonance tuning nanoprobe (TMRET) in conjunction with image-guided application	Nephrogenic systemic fibrosis (NSF) Nervous system abnormalities Poor biocompatibility Ineffective targeting	47, 50–53

GBCAs have been utilized in MRI scans to improve diagnostic accuracy and provide a more realistic depiction of diseases.[55] Gadolinium is a heavy metal with a 3^+ charge and seven unpaired electrons. At low concentrations, the binding of Gd^{3+} enhances the relaxation time of neighboring protons in a magnetic field, thereby enhancing the quality of the image, which is crucial for distinguishing different tissues in disease diagnosis. Although gadolinium is not naturally present in human tissues, it is highly valuable for enhancing the MRI signal due to its exceptional paramagnetic properties.[56] One of the main concerns regarding these contrast agents (CAs) is the potential accumulation of gadolinium in the brain and the subsequent development of systemic nephrogenic fibrosis due to frequent MRI contrast administration.[57] Evidence suggests that the intravenous administration of GBCAs increases the risk of neurotoxic side effects. Animal studies have shown that higher intrathecal doses of GBCAs, such as gadodiamide and Gadopentetate dimeglumine, can lead to neurotoxicity symptoms, including myoclonus, gait disruption, tremors, ataxia, and seizures. These side effects are associated with histopathologic abnormalities such as astrocytic hypertrophy, loss of oligodendroglia and eosinophilia that occur at doses equivalent to 5–15 mol gr^{-1} of brain tissue. Several case studies involving humans have demonstrated the neurotoxic effects of intrathecal injection, often resulting from unintentional overdoses. These cases have presented symptoms such as bewilderment, global aphasia, stupor, vomiting, rigidity, hypertension, and seizures.[58]

Due to the toxicity and possible negative long-term effects of Gd-based CAs building up in the body, new approaches that increase the safety of Gd- based MRI CAs can be employed, such as encapsulating Gd based contrasts in liposomes, binding free Gd ions to organic ligands and forming Gd^{+3} chelates, and integrating Gd into different nanocarriers.[59,60]

In a study, Setiawan *et al.* developed gold nanorods coated with functionalized PAMAM dendrimers tailored with Gd-DOTA molecules and poly (ethylene glycol) for biocompatibility and MR imaging attributes. The modified dendrimer with Gd-DOTA can effectively reduce the rotational motion of Gd ions, acting as a macromolecular contrast agent. Additionally, HER2-specific antibodies were conjugated to target cancer cells expressing HER2. The nano-hybrids exhibited T1w relaxation and MR imaging characteristics similar to commercially available MR contrast agents. Gadolinium, used as a diagnostic agent, helped suppress tumor growth and improve survival rates in mice with breast tumors undergoing photothermal therapy using gold nanoparticles. These synthesized nanoparticles show promising results as targeted theranostic contrast agents for breast cancer treatment.[61]

The positioning of gadolinium atom(s) and their potential interactions with water molecules in the target tissue significantly affect the ability of GBCAs to produce contrast. The tight binding of gadolinium ions to the carrier scaffold can be disadvantageous due to the structural properties of the scaffold components, ultimately reducing the interaction between Gd^{3+} and water molecules in the surrounding tissue. In this regard, Patil and colleagues conducted a study where they developed gadolinium conjugates with peptides and antibodies, both in single-arm and multi-arm ("star") configurations, to investigate the impact of gadolinium distance. Gadolinium-DOTA, intermediates, and targeting agents such as antibodies and peptides were used as amides and thioethers. The performance of this complex was evaluated for tumor imaging in a mouse glioma model with MRI. The distance between the polyanion and Gd-DOTA on linear and branched PEG influenced the Gd relaxivity rate based on length and branching degree. Gadolinium conjugates with Ab showed higher relaxivity and improved contrast for differentiating brain tumors *via* MRI compared to the commercial MultiHance contrast agent.[62]

3.2. Manganese-based antibody conjugates as T1 MRI contrast agents

Manganese-based contrast agents (MnCAs) have been proposed as a safer alternative to GdCAs. Mn^{2+} exhibits rapid water exchange a prolonged electronic relaxation time, and possesses five unpaired d electrons. These attributes make it favorable for enhancing T1 contrast. Manganese is a biogenic and indispensable element ubiquitously present in almost all tissues. It is crucial in bone formation, brain health, and cellular and physiological (especially mitochondrial) processes. It is vital for metabolizing proteins, amino acids, carbohydrates, and lipids. It also contributes to protein digestion, liver glycogen storage, and cholesterol and fatty acid synthesis. However, most ligands offer Mn^{2+} lower thermodynamic stability than other transition metals in the Irving–Williams family, resulting in limited crystal field stabilization.[63]

Recently, Han *et al.* synthesized carbon nanosheets doped with nitrogen and manganese (Mn-N-CNSs) and combined them with an anti-HE4 antibody (anti-HE4@Mn-N-CNSs). This combination allowed for precise and targeted fluorescence and MRI of ovarian cancer. The prepared system exhibited excellent colloidal stability, remarkable aqueous dispersity, impressive optical properties, and a higher longitudinal relaxivity rate (r_1 = 10.30 mM^{-1} s^{-1}). The nanoprobe demonstrated enhanced and targeted MR contrast effects in both tumor-bearing mice model and ovarian cancer cells, according to its higher r_1 relaxivity. *In vitro* experiments results, indicated that the synthesized nanotheranostics produce greater signal intensity in T1-weighted images than that commercial Gd-DTPA (Fig. 1).[64]

Manganese is a crucial component of certain receptors and enzymes. Due to its high biocompatibility and low toxicity, manganese oxide (MnO) has been widely utilized as a nano-agent in various studies. Manganese oxide nanoparticles (MONPs) are designed as T1 contrast agents for MRI, with different nanoplatforms such as core–shell-

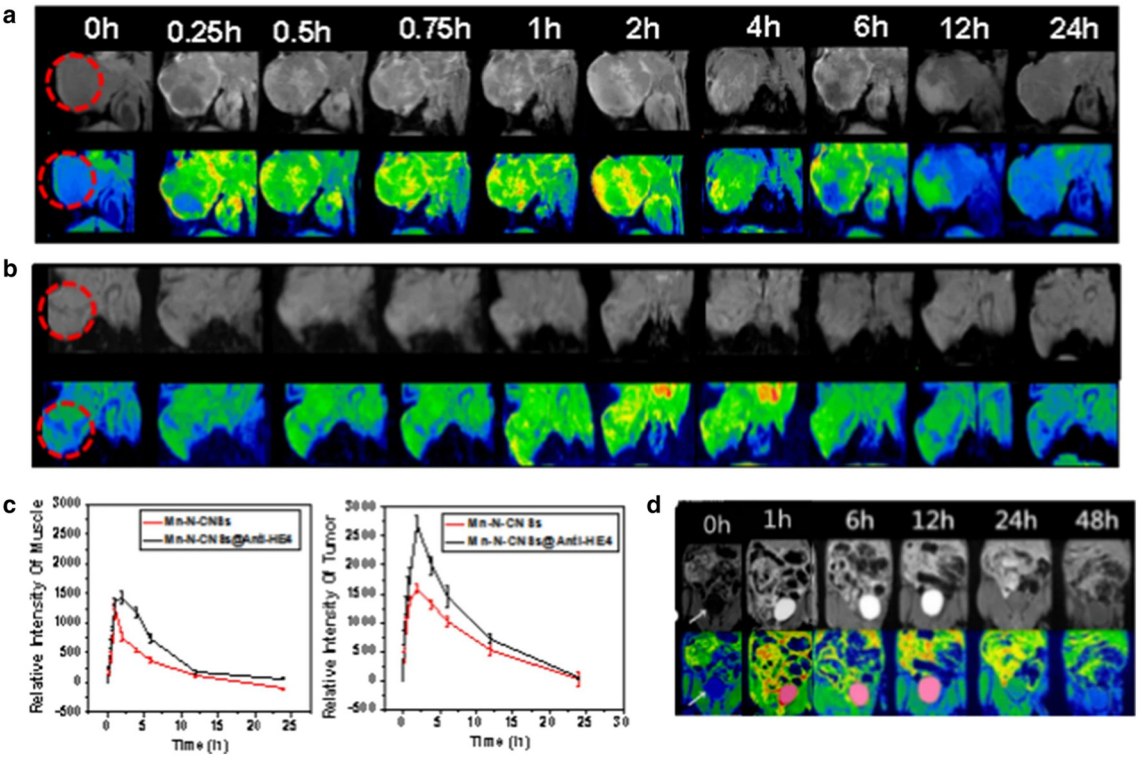

Fig. 1 T1-weighted MRI images of mice with a) anti-HE4@Mn-N-CNSs nanoprobe and b) Mn-N-CNSs at time intervals are displayed above. Corresponding pseudo-color images are presented below. c) Tumors can be observed within the red circles, along with the signal strength in the muscles and tumors. d) Additionally, T1-weighted and related pseudo-color MR images depict mice before and after administering anti-HE4@Mn-N-CNSs. The gall bladder is indicated by the white arrows.[64]

based MONPs, ratchet-kind MONPs, and MONPs dispersed uniformly in a mesoporous framework. In a study by Du *et al.*, manganese oxide–mesoporous silica nanoparticles (Mn-MsNPs) were developed and then conjugated with Cy7 and PSA antibody. This resulted in the creation of a multimodality Cy7-Msn-Mn-PSA system for diagnosing prostate cancer. The nanoparticles exhibited stability and showed enhanced T1 relaxivity. Importantly, *in vitro* experiments demonstrated that the targeted NPs accumulated in prostate cancer cells rather than normal cells. *In vivo*, experiments further confirmed the distribution of the targeted Cy7-Msn-Mn-PSA system in tumor tissues, as indicated thru T1 and strong optical signals.[65]

Moreover, Zhan *et al.* created Mn_3O_4 nanoparticles in a recent study. They conjugated the nanoparticles to the radioisotope copper-64 and the anti-CD105 antibody TRC105 for tumor vasculature-targeted imaging in mice. The Mn-conjugated NPs (^{64}Cu–Mn@PEG-TRC105) demonstrated great radio stability and numerous specificities for tumor targeting. The Mn_3O_4-conjugated NPs also showed favorable features for T1-improved imaging and lower toxicity.[66]

3.3. SPION-based antibody conjugates as T2 contrast agents

Superparamagnetic iron oxides (SPIO) have long been extensively studied as MRI contrast agents due to their exceptional magnetic properties and biocompatibility. Compared to GBCAs, SPIO-based NPs exhibit higher proton relaxation efficiency and slower renal clearance, enabling their use at lower doses. It is worth noting that iron is an essential element for the human body, and thus, it follows metabolic pathways.[67] Although iron oxide (Fe_2O_3 and Fe_3O_4) nanoparticles are biocompatible, biodegradable, and non-toxic, they are detected and eliminated by the body's immune processes and directed toward the primary elimination channels shortly after *in vivo* delivery. Consequently, in therapeutic applications or clinical diagnostics, active clearance and competition for nanoparticle distribution in blood or specific organs occur.[68] T2-weighted MRI contrast agent SPIO particles, widely investigated as a diagnostic tool for various disorders, function by shortening the T2 relaxation time in MRI. Some examples, such as ferumoxide and ferucarbotran, have already received clinical approval. Researchers have demonstrated that ultrasmall SPIO particles with a diameter of less than 4 nm, owing to their abundance of surface paramagnetic iron ions capable of reducing the T1 of nearby water protons, may serve as a T1 contrast agent[69] (Table 3).

Multiple studies have demonstrated that the concentration of SPIONs in the tumor site may increase after conjugation with scFvs (single-chain variable fragments), antibodies, and peptides. This rise could improve the image quality of certain solid tumors such as breast cancer, glioblastoma, prostate tumors, and lung malignancies. Lu

Table 3 Applications and relevant examples of antibody nanoconjugates in MRI

Type of cancer	Material type	Antibody	Targeting moieties	Type of contrast agent	Ref.
Prostate	SPION: molday ION rhodamine-B carboxyl	Mouse monoclonal antibody (muJ591)	PSMA	T2	70
Pancreatic	SPIONs	Anti-plectin-1	Plectin-1	T2	71
Prostate	SPION	J591 mAb	PSMA	T2	72
Breast	MONs	Anti-CD105 antibody TRC105	CD105	T1	73
Glioblastoma	SPIONs	Anti-EGF rabbit polyclonal antibody	EGFR	T2	74
Breast	Iron oxide	Anti-Her2/neu antibody	HER2	T2	75
Hepatocellular carcinoma	SPIONs	Anti-AFP and anti-glypican 3	AFP and GPC3 antigens	T2	76

et al. employed a scFv targeting EGFR (epidermal growth factor receptor) with Fe_3O_4/Au NPs (iron oxide–gold nanoparticles) to create an EGFR-specific MRI bio-probe (scFv@Fe_3O_4/Au) for detecting non-small cell lung cancer (NSCLC). EGFR-positive tumor cells showed significant uptake of scFv@ Fe_3O_4/Au *in vitro*. The MRI signal in T2-weighted images (T2w) in EGFR-positive tumors was considerably reduced *in vivo* after scFv@ Fe_3O_4/Au injection (Fig. 2).[77]

Recently, Zarghami *et al.* developed a MRI contrast agent by conjugating anti-ALCAM antibody to iron oxide micro-particles (MPIO). This agent was designed to detect endothelial ALCAM expression *in vivo*. To further validation, the researchers conducted a proof-of-concept study using mouse models with brain metastasis induced by intracardial injection of brain-tropic human melanoma cells, breast carcinoma and lung adenocarcinoma. The complex was administered intravenously at different time intervals, and the resulting MRI signal in T2*w images showed a decrease (Fig. 3).[78]

To extend the lifespan of SPIONs in circulation and minimize adverse effects, one can encapsulate them using biocompatible polymers like polyethylene glycol aldehyde (PEG-aldehyde) and PLGA. Recently Salehnia *et al.* prepared an anti-EGFR-conjugated SPIONs as targeted MRI contrast agents for imaging of lung cancer cells that exhibiting EGFR overexpression. In this study, the Fe_3O_4-loaded PLGA-PEG NPs were synthesized using a modified water-in-oil-in-water double emulsion technique. Furthermore, the EGFR antibody was conjugated to the surface of the SPIONs. They utilized a T2w spin echo imaging sequence with a TE of 22 ms and TR of 4000 ms to assess the contrast effect of various NP solutions. The resulting nanoprobes exhibited a reduction in MRI T2 relaxation time, coupled with an augmentation in Fe concentration. These nanoprobes have the potential to function as T2w negative contrast agents for EGFR detection.[79] In a study, Fe_3O_4@Au nanoparticles coated with PEG and trastuzumab (TZ) were synthesized as an MRI probe. The team evaluated the prepared system's cytotoxicity, blood compatibility, relaxivity, colloidal stability, and *in vivo* MR contrast enhancement. The nanoprobe enhanced the negative signal in MRI and showed potential for cancer detection.[80]

Li *et al.* developed a novel contrast agent for dual-mode imaging of HER2-positive breast cancer, combining ultrasound (US) and MR techniques. This was achieved by incorporating Fe into hollow silica nanoparticles (HS-Fe NPs), subsequently modified with anti-HER2 antibody. The distribution of nanoparticles in animal model was examined. The results showed that the complex produced a negative contrast in T2w MR imaging and significantly enhanced the US signal.[81]

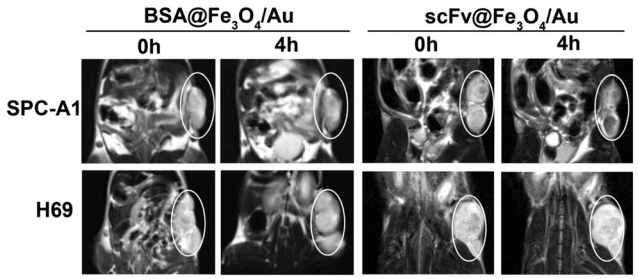

Fig. 2 Signal intensity change in T2w MR images was demonstrated through the use of two synthesized nanoparticles (BSA@Fe_3O_4/Au and scFv@Fe_3O_4/Au) in mouse xenografts with two lung cancer tumors (SPC-A1 and H69). The SPC-A1 xenograft mice treated with scFv@Fe_3O_4/Au showed a reduction in tumor signal. Furthermore, 4-hour delayed images of the spleen, liver, and kidney of tumor mice indicated a significant decrease in SNR in both types of NPs.[77]

4. T1/T2 dual-mode antibody-based CAs in MRI

Due to the unfortunate fact that most clinically approved T1 and T2 contrast agents (CAs) for MRI diagnosis have inherent drawbacks related to imaging ambiguities, MRI artifacts, and health risks, there has been significant attention towards the development of strategies for T1/T2 dual-mode contrast agents (DMCAs) in recent times, particularly when the biological targets are small, in addition to the challenges with image matching brought on by moving the imaging object and the disparities arising from various depth penetrations and spatial/temporal resolutions of several imaging strategies.[82] These DMCAs have the potential to

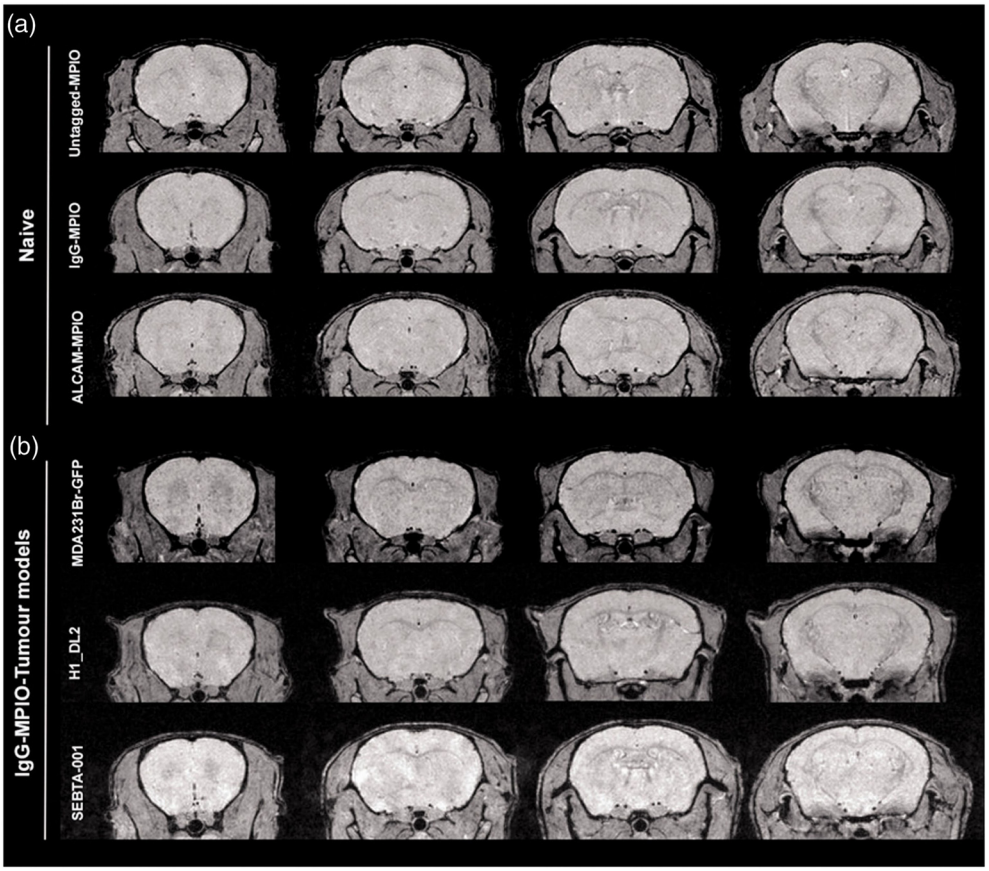

Fig. 3 Analyzing the specificity of ALCAM-MPIO in mice: a) typical T2*-weighted MGE3D coronal images of untagged ProMagTM carboxylic MPIO, ALCAM-MPIO, or IgG-MPIO injections in naive mice. Only a few hypointense voxels related to MPIO were observed in this control group. b) Typical T2*-weighted MGE3D coronal images were taken on days 21 (H1_DL2, MDA231Br-GFP) and 42 (SEBTA-001) from tumor-bearing animals injected with non-specific IgG-MPIO. Once again, only a few hypointense voxels were observed in these mice.[78]

produce highly accurate diagnostic images with complementary advantages.[64] However, synthesizing T1/T2 DMCAs on a single platform remains challenging. Before DMCAs can be clinically utilized, it is crucial to consider their ease of synthesis, chemical stability, non-toxicity, and favorable biodistribution (lower uptake in the liver and kidneys).[83] It is imperative to develop dual-mode contrast agents with improved biocompatibility because, as previously mentioned, contrast agents based on Gd or Mn can cause respectively, renal systemic fibrosis and nervous system abnormalities, in some patients. This has limited the broader application of these agents.[50] Recently, Marie-Josée Jacobin-Valat *et al.* created PEGylated dextran/iron oxide nanoparticles which labeled with rhodamine for diagnosing the early stages of atherosclerosis. Considering the role of p-selectin in the initial loose contact between the vessel wall and platelets, this contrast agent was conjugated with p-selectin antibody. MRI results demonstrated 50% decrease in signal of T2 and T1 values. In addition, an *in vivo* study was performed and ApoE mice (the most widely used pre-clinical model of atherosclerosis) were subjected to MRI imaging. The results showed a hypo-signal at 4.7 T which indicates the accumulation of nanoparticles in atherosclerotic plaques.[84] The results of this study show the high capacity of targeting MRI dual mode contrast agents with antibody to obtain images. In the reviewed studies, no T1/T2 dual mode antibody-based MRI contrast agents have been reported for the diagnosis and imaging of cancers. Considering the unique features of antibodies in targeting nanoparticles, this topic can be of interest to researchers.

5. Antibody-conjugated NPs as CT contrast agents

Furthermore, because CT scans have limited effectiveness in assessing soft tissues and tumors, contrast agents are used in CT imaging to enhance their capabilities. This technique is referred to as contrast-enhanced CT. Chemical elements with higher atomic numbers, such as bismuth, iodine, gold, tantalum, silver, and platinum, exhibit excellent performance in CT imaging due to the photoelectric effect.[85,86] This effect is influenced by the atomic number and the binding energy of the K-shell electron, which primarily contributes to X-ray attenuation. For further details, refer to Table 4.

Table 4 Advantages of chemical elements with K-edges in the X-ray spectrum and higher atomic numbers

Elements	Chemical symbol	Advantages	Atomic numbers	Ref.
Silver	Ag	Stable, biocompatible, no acute toxicity, higher contrast	$Z = 47$	87
Platinum	Pt	Workable surface functionalization of thiol–metal bonds, enhanced X-ray absorption, and easy synthesis control	$Z = 78$	88
Tantalum	Ta	Superb biocompatibility, elevated X-ray attenuation coefficient, easily modifiable surface chemistry, prolonged circulation, exceptional safety profiles, and superior contrast performance	$Z = 73$	89
Gold	Au	High atomic number and density, biocompatible	$Z = 79$	90
Bismuth	Bi	Suitable antioxidant activity, high physiological stability, low toxicity, natural degradability, long circulation time, high CT contrast efficacy	$Z = 83$	91
Iodine	I	High-resolution images with a lower concentration, half-life in various organs are longer than the time it spends there, which makes it easier to monitor vital organs like the heart and blood vessels to look for abnormalities	$Z = 53$	92

5.1. Single-metal antibody based CT contrast agents

To enhance image contrast in CT scans, an effective imaging agent is required. This agent should possess low toxicity, exhibit high absorption in the target tissue, and have a prolonged circulation time in the bloodstream. Various materials, such as bismuth, iodine, gold, tantalum, and platinum, are employed for this purpose. Among these, gold nanoparticles (AuNPs) have gained significant attention in cancer diagnosis and treatment due to their inherent properties. *In vivo*, AuNPs demonstrate exceptional stability, are nonimmunogenic, and exhibit minimal toxicity. The preferential accumulation of AuNPs in tumors, either through passive targeting (also known as the EPR effect) or active targeting, may contribute to improved sensitivity in imaging diagnosis and therapeutic efficacy. Compared to iodine-based contrast agents, which are associated with renal toxicity and rapid renal clearance, AuNPs offer a more desirable option for enhancing CT imaging. This is due to their 2.7 times higher X-ray mass attenuation.[93]

Kimm *et al.* recently created cmHsp70.1-AuNPs, a gold nanoparticle-functionalized antibody, which specifically targets the plasma-membrane heat shock protein 70 (Hsp70) for multimodal imaging of tumors. Microscopic analysis of tumor cell lines *in vitro* revealed the presence of cmHsp70.1-AuNPs within their cytosol. In preclinical models of tumor-bearing mice, the biodistribution and intra-tumoral accumulation of AuNPs were examined 24 hours after intravenous injection. The results demonstrated these antibody-conjugated AuNPs' potential for radiotherapeutic interventions and tumor detection (Fig. 4).[94]

Under normal physiological conditions, gold nanoparticles tend to aggregate easily, which hinders the enhanced permeability and retention (EPR) effect and can lead to vessel embolism. In order to enhance the EPR effect, nanoparticles need to have sufficient blood retention. To accomplish this, nanoparticles' surfaces can be modified by adding polymers like polyethylene glycol (PEG) chains. In a study conducted by Nakagawa *et al.*, gold nanoparticles with PEG chains attached to their surfaces were developed to improve blood retention. These nanoparticles were then linked to a cancer-specific antibody using the terminal PEG chains. The distribution of the synthesized gold nanoparticles was analyzed using CT imaging after injecting them into mice with tumors. The results showed that the conjugation of a specific antibody against the tumor, along with a slight variation in particle size, enhanced the targeted accumulation of the gold nanoparticles in the tumor (Fig. 5).[95]

In a recent study, Ghaziyani *et al.* synthesized a novel contrast agent using gold to enhance the CT scan's capability to identify cancer cells exhibiting higher CD24 expression. To modify the gold nanoparticles, they incorporated both short PEG (HS-PEG-COOH) and long PEG (HS-PEG-CH3O) chains. These chains were then conjugated with CD24 antibodies, resulting in CD24-PEGylated Au-NPs. The findings indicate that the developed nano contrast successfully detected cancer cells expressing the CD24 antibodies.[96]

Dendrimers are a type of molecule that can be utilized as a surface modifier for nanoparticles due to their enhanced

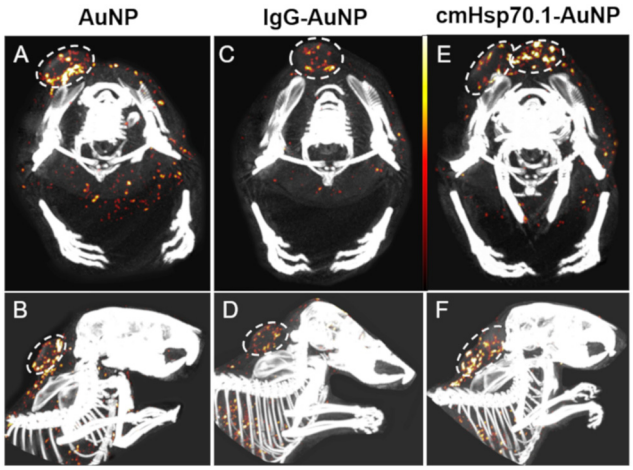

Fig. 4 Tumors detected using spectral-CT. The upper row (A, C, E) displays an axial cross-section, while the bottom row (B, D, F) shows a sagittal projection. The concentrations of AuNPs range from white (13.5 mg mL^{-1}) to red (10 mg mL^{-1}) to black (6.5 mg mL^{-1}). The spectral CT images depict mice injected with AuNPs (A and B), IgG-AuNPs (C and D), and cmHsp70.1-AuNPs (E and F).[94]

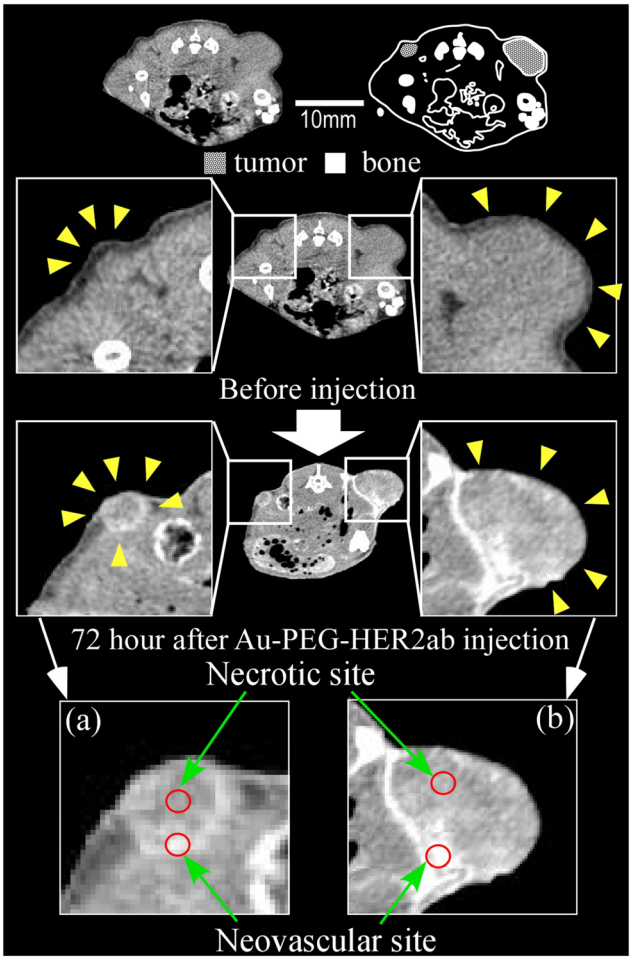

Fig. 5 Contrast effect observed after injecting 15 nm Au-PEG NPs into a tumor; unlike the 30-nm Au-PEG, the Au-PEG NPs could visualize a small mouse microtumor just a few millimeters away. The images on the left and right show large tumors and microtumors, respectively. The yellow arrowheads indicate the tumor region. a) The neovascular and necrotic sites had CT values of 72 HU and 244 HU, respectively. b) The neovascular and necrotic sites had CT values of 60 HU and 280 HU, respectively.[95]

stability of conjugated substances and improved biocompatibility, in contrast to linear-shaped polymers.[97] In a study, Chen *et al.* developed a bi-modal, HER-2-specific dendrimer conjugate to enhance the detection potential of MRI and CT for HER-2-positive breast cancer. The contrast agent for the nanoparticle is created by combining PAMAM G5 dendrimers, chelated gadolinium, encapsulated gold NPs, and an anti-human HER-2 antibody. When injected intravenously into mice with HER-2-positive breast cancers, this NP increases CT contrast and resolution by a factor of two and increases MRI signal intensity by 20%.[98]

Studies have shown that adding small particles to NPs increases their retention on tumors while adding them to large nanoparticles (>100 nm) is not beneficial. On the other hand, using targeted molecules like immobilized proteins, particularly antibodies, makes the NPs recognizable by the immune system. Therefore, it is preferable to use small molecules such as folic acid (FA), aptamers, or antibody fragments without the FC domain as alternatives to full antibodies. Ashton, *et al.* have focused on developing a gold NP contrast agent that targets the EGFR expressed on the surfaces of several lung adenocarcinomas' cells. To evaluate the effectiveness of tumor targeting, a comparison was conducted among three contrast agents: NPs conjugated with cetuximab, non-targeted NPs, and NPs conjugated with a single-domain anti-EGFR antibody-derived from llamas. The smallest identified antibody segments are VHH domains that maintain target specificity. The results showed that all three contrast agents could be effectively used for tumor imaging by CT and vascular imaging. Studies have shown that VHH antibodies are expected to have superior targeting abilities compared to full-sized antibodies. However, this study revealed a contrary result. C225 (cetuximab)-AuNPs exhibited significantly increased tumor uptake due to their distinctive targeting mechanism (Fig. 6).[99]

Bismuth has various biological applications due to its non-toxic nature and affordability, coupled with its remarkable characteristics.[100] Bi-based contrast compounds have gained significant attention for their versatility and biocompatibility. With its high atomic number (Z = 83), bismuth (Bi) exhibits a relatively high X-ray attenuation coefficient (5.74 cm^2 kg^{-1} at 100 keV). Consequently, Bi agents can be effectively used as contrast agents in X-ray imaging. However, pure Bi nanoparticles (NPs) tend to be unstable, oxidizing quickly to form Bi hydrate and degrading, resulting in poor performance. Therefore, enhancing the stability of Bi NPs is crucial.[101] Recently, Li *et al.* developed core–shell NPs consisting of bismuth sulfide@mesoporous silica (Bi_2S_3@mPS) for targeted image-guided treatment of HER-2 positive breast cancer. To synthesize these NPs, rod-like Bi_2S_3 NPs decorated with polyvinylpyrrolidone are encapsulated with mPS layer. The NPs are then loaded with doxorubicin and chemically conjugated with trastuzumab, a monoclonal antibody that targets HER-2 overexpressed breast cancer cells. The findings of this study demonstrate the potential of Tam- Bi_2S_3@mPS NPs as a superior contrast enhancement probe for computed tomography.[102]

Iodine is a potential contrast agent for CT scans. It is commonly used to highlight specific organs, blood vessels, and tissues in modern medicine. Contrast agents containing Iodine can improve the accuracy of diagnostic CT scans. However, they have also been associated with acute kidney injury (AKI) and thyroid dysfunction.[103] In a study by Su *et al.*, iodine-doped carbon quantum dots (I-CQDs) were prepared. These I-CQDs were coupled with a targeted molecule, cetuximab, resulting in I-CQDs-C225. Bio-imaging results showed that this system could specifically enter HCC827 cells (a lung cancer cell line with overexpression of EGFR). The complex demonstrated higher sensitivity and excellent spatial resolution, making it suitable as a targeted CT bimodal imaging/fluorescence probe.[104]

Another example is tantalum oxide-based nanoparticles (TaOx NPs), which possess notable characteristics such as

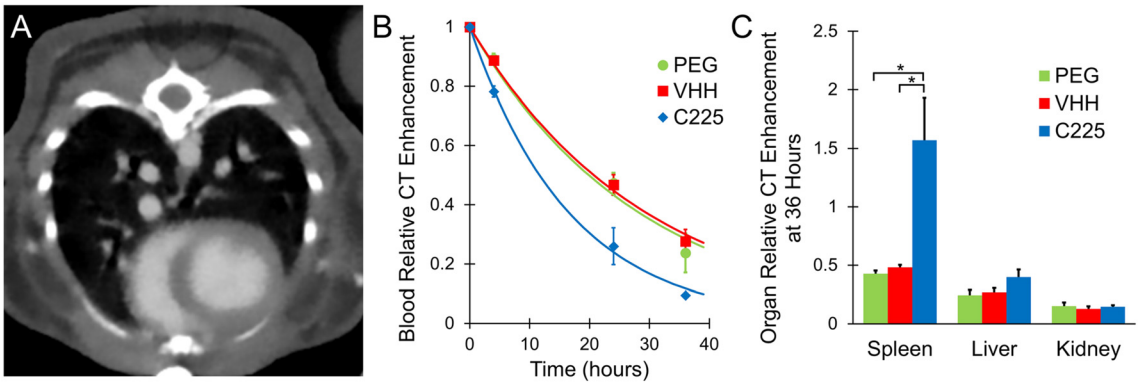

Fig. 6 The CT number was increased, indicating enhanced contrast in the CT image of healthy mice following the injection of AuNP contrast agents. An axial projection of the CT scan with contrast enhancement after injecting VHH-AuNPs is displayed (A). The increase in CT number was compared by injecting three different types of contrast agents in a time sequence, and NPs generated an exponential fitting curve. All NPs exhibited an exponential decrease in concentration. The half-life of C225 was significantly shorter than that of VHH-122 or PEG (B). Three types of synthesized contrast agents were used to compare the delayed absorption over 36 hours to the initial few minutes in three tissues: spleen, liver, and kidney. C225 demonstrated a higher accumulation in the spleen compared to VHH-122 or PEG (C).[99]

excellent biocompatibility, a high X-ray attenuation coefficient, and easily adjustable surface chemistry. These properties make them highly promising CAs for CT imaging. Regarding contrast enhancement, prolonged circulation in the body, and good safety profiles, TaOx NPs outperform commercially available contrast agents.[89] Platinum (Pt)-based NPs exhibit the greatest potential as optimal CT imaging contrast agents compared to other flexible inorganic CAs. This is due to their ability to be easily controlled during manufacturing, higher X-ray absorption, and the possibility of surface functionalization through thiol–metal bonds (Table 5).[88]

5.2. Bimetallic/polymetallic antibody based CT contrast agents

Combining two distinct metals results in the formation of bimetallic NPs (BNPs). In comparison to monometallic nanoparticles, BNPs have garnered significant attention from the scientific and technological community due to their superior features.[110] BNPs can have a variety of shapes depending on the kinds of metal that are used. Numerous studies have detailed how to coat these particles with a broad range of compounds for various purposes, including silica, polymers, liposomes, and dextran.[111] Due to the possibility of examining the unique roles of two or more metal elements, the synthesis of bimetallic core–shell NPs has also garnered a lot of interest.[112] Due to their special physical characteristics (such as the large surface area, mobility, and the quantum effect) as well as their chemical, optical, mechanical, catalytic thermal, and magnetic qualities, bimetallic NPs have attracted increased attention in recent years. Application for bimetallic NPs include biomedical, nanomedicine, biosensors, imaging, gene/drug delivery, among other domains.[113] Utilizing the intrinsic qualities of the nanometals in BNPs, they can be used as contrast agents while imaging cancer. Furthermore, these can be joined with treatment plans integrated into the same nanoparticle to produce a multipurpose nanoplatform known as a theranostic.[114] Also polymetallic NPs are made from a combination of more than two distinct metals. Polymetallic NPs are an interesting avenue to study. They essentially combine the benefits of a low metal/ligand mass ratio with a high molecular weight.[115] In a study, Song Zhang *et al.* developed Bimetallic core/shell Fe_2O_3/Au nanoparticles as a promising candidate dual-mode contrast agents for CT and MRI imaging. In comparison to the other hybrids examine in this study, the hybrids formed after three Au seeding cycle are the favored choices for MRI and CT applications due to their comparatively high R_2 relaxivity (95 mM^{-1} s^{-1}) and X-ray attenuation (1.87 times that of iodine).[112] Aviv *et al.* focused on developing novel x-ray contrast agent Bi2O3/HSA (human serum albumin) core–shell NPs. In order to stabilize the particles in an aqueous phase and to bind different bioactive reagents, including antibodies, to their surface for molecular imaging applications, the HSA shell is required. *In*

Table 5 Applications and relevant examples of antibody nanoconjugates in CT

Type of cancer	Material type	Targeting moieties	Ref.
Lung squamous cell carcinoma (SCC)	Gold nanoclusters (AuNCs)	Dsg-3 antibodies	105
Breast cancer	Gold NPs	Trastuzumab (TZ)	106
Prostate cancer	Gold NPs	PSMA	107
Breast cancer	Gold NPs	Anti-human HER-2	108
Prostate cancer	Gold NPs	PSMA	109

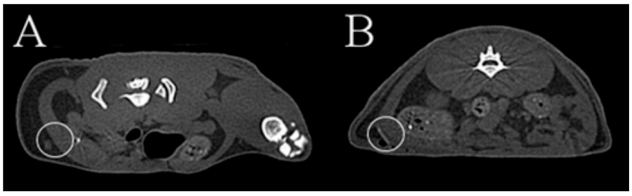

Fig. 7 Before (A) and 24 h after (B) a subcutaneous injection of 2 mL of the dispersion of Bi2o3/HAS core–shell NPs in 5% dextrose aqueous solution, micro CT images of the rats.[116]

vivo and *in vitro* CT imaging was done. The radiopaque core made of Bi_2O_3 allows the core–shell NPs to improve CT signals (Fig. 7).[116]

In another study, Fei He *et al.*, for the first time prepared uniform bimetallic Au_1Bi_1–SR NPs with photodynamic, CT imaging, and photo thermal capabilities. The Bi element can be utilized as an efficient developer to increase the signal contrast in CT imaging because to its high X-ray attenuation coefficient. The performance of NPs as an *in vivo* and *in vitro* CT contrast agents was studied. NPs were injected to mice intratumorally and the results showed the significant increase in CT signal of tumors (Fig. 8).[117]

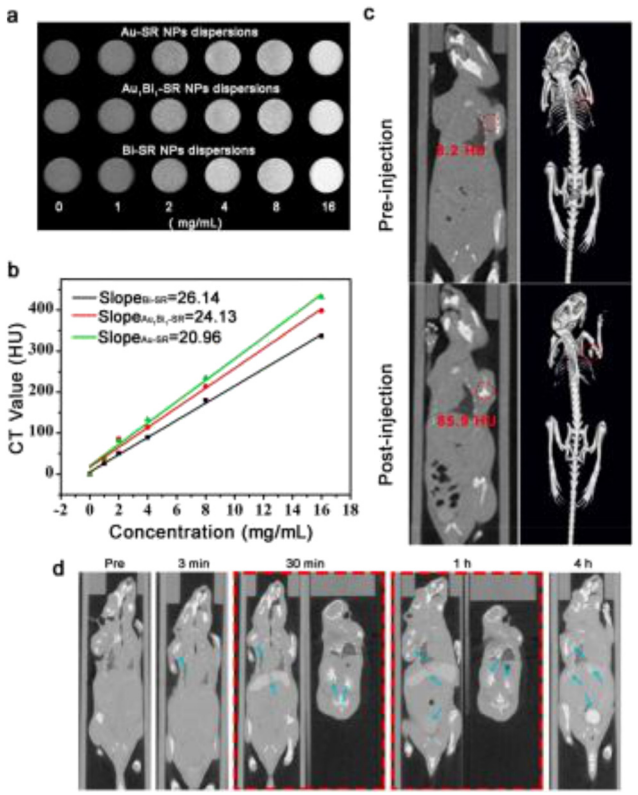

Fig. 8 a) CT images of, Au_1Bi_1–SR NPs, Bi–SR NPs and Au–SR NPs *in vitro*. b) HU value and concentration curves of Au_1Bi_1–SR NPs solution. c) 3D images and *in vivo* CT images of a tumor-bearing mouse: pre and post injection (top and bottom respectively) of the Au_1Bi_1–SR solution in tumor cite. d) *In vivo* CT images of intravenous injection of Au_1Bi_1–SR solution at various injection time.[117]

6. Conclusions and future perspectives

Imaging probes developed using nanomedicine as a foundation are highly effective in identifying cancer cells. Though, finding the perfect ligand with optimal performance and efficient binding characteristics is a challenging task.[118,119] Numerous preclinical studies in oncology have demonstrated the enhanced cancer detection and monitoring capabilities of antibody-based imaging probes. When an antibody and NP are combined, the characteristic of the NP are combined with the antibodies' capacity to recognize antigens in a particular and targeted manner. Furthermore, two of the main benefits of employing antibody –conjugated NPs may be the enhancement of intracellular stability and cellular uptake. However, commercial development is still unrealistic due to the high concentration of antibody-labeled NPs needed to produce a signal with sufficient contrast.[120] These probes offer other impressive benefits, including low toxicity, high specificity, fewer side effects, good biodistribution, improved selectivity in antigen binding, favorable pharmacokinetic properties, and extended blood circulation time. Furthermore, the required doses for imaging agents based on antibodies are often lower than those used for therapeutic purposes. As a result, the toxicity profile typically refers to non-dose-dependent events such as immunological reactions.[121] Although small animals have been extensively studied, clinical translation, especially in complex multimodal imaging, remains a limitation of these imaging techniques.[122] This may be due to the complexity of developing imaging probes, safety concerns, high costs, difficulty anticipating their effects and interactions with biological systems, and significant variations between human cancer patients and animal models.[122–124] Image analysis, which is more complicated than traditional medical imaging, is another drawback. Furthermore, certain contextual factors, such as interface competition, access to tissues *via* blood vessels, and efficient clearance by the reticuloendothelial system, may impact clinical translation. It should be noted that in a selected period for searching related articles, no study was reported on the conjugation of antibody with T1/T2 dual mode contrast agents in MRI and bimetallic and polymetallic CT contrast agents for cancer detection, therefore, the reports in this article are only have investigated the contrast properties of this nanoparticle without antibody conjugation. It seems that conjugation of antibody with this types of contrast agents can enhance their unique features and it is suggested to be investigated in future studies. However, antibodies could target ligands for NPs-based diagnostics, and the use of antibody-based methods in clinical cancer imaging will significantly advance cancer detection and monitoring in the future. Finally, a thorough assessment of these new technologies will be required soon to improve cancer detection.

Data availability

Data available on request.

Conflicts of interest

The authors declare no conflict of interest.

Acknowledgements

This study was supported by the Research Center for Pharmaceutical Nanotechnology, Tabriz University of Medical Sciences (Grant No. 71051).

References

1 X.-J. Chen, X.-Q. Zhang, Q. Liu, J. Zhang and G. Zhou, *J. Nanobiotechnol.*, 2018, **16**, 1–17.
2 P. Lancellotti, M.-L. Nguyen Trung, C. Oury and M. Moonen, *Eur. Heart J.*, 2021, **42**, 110–112.
3 O. Y. Ibhagui, D. Li, H. Han, G. Peng, M. L. Meister, Z. Gui, J. Qiao, M. Salarian, B. Dong and Y. Yuan, *Chem. Biomed. Imaging*, 2023, **1**, 268–285.
4 L. P. Pushparaj and S. Sathya, *Ir. Interdiscip. J. Sci. Res.*, 2021, **5**, 07–17.
5 Z. Sun, W. Chen, W. Sun, B. Yu, Q. Zhang and L. Lu, *CCS Chem.*, 2021, **3**, 1242–1257.
6 J.-s. Choi, S. Kim, D. Yoo, T.-H. Shin, H. Kim, M. D. Gomes, S. H. Kim, A. Pines and J. Cheon, *Nat. Mater.*, 2017, **16**, 537–542.
7 A. Mirzaei, A. R. Jalilian, A. Aghanejad, M. Mazidi, H. Yousefnia, G. Shabani, K. Ardaneh, P. Geramifar and D. Beiki, *Nucl. Med. Mol. Imaging*, 2015, **49**, 208–216.
8 A. Aghanejad, A. R. Jalilian, S. Maus, H. Yousefnia, P. Geramifar and D. Beiki, *Iran. J. Nucl. Med.*, 2016, **24**, 29–36.
9 A. Aghanejad, A. R. Jalilian, Y. Fazaeli, B. Alirezapoor, M. Pouladi, D. Beiki, S. Maus and A. Khalaj, *Sci. Pharm.*, 2014, **82**, 29–42.
10 P. Siminzar, M. R. Tohidkia, E. Eppard, N. Vahidfar, A. Tarighatnia and A. Aghanejad, *Mol. Imaging Biol.*, 2023, **25**, 464–482.
11 D. Zhi, T. Yang, J. Yang, S. Fu and S. Zhang, *Acta Biomater.*, 2020, **102**, 13–34.
12 V. Mittelheisser, P. Coliat, E. Moeglin, L. Goepp, J. G. Goetz, L. J. Charbonnière, X. Pivot and A. Detappe, *Adv. Mater.*, 2022, 2110305.
13 X. Lin, A. O'Reilly Beringhs and X. Lu, *AAPS J.*, 2021, **23**, 1–16.
14 S. Schuerle, M. Furubayashi, A. P. Soleimany, T. Gwisai, W. Huang, C. Voigt and S. N. Bhatia, *ACS Synth. Biol.*, 2020, **9**, 392–401.
15 C. Nicolescu, A. Schilb, J. Kim, D. Sun, R. Hall, S. Gao, H. Gilmore, W. P. Schiemann and Z.-R. Lu, *Chem. Biomed. Imaging*, 2023, **1**, 461–470.
16 F. Maghsoudinia, M. B. Tavakoli, R. K. Samani, S. H. Hejazi, T. Sobhani, F. Mehradnia and M. A. Mehrgardi, *Talanta*, 2021, **228**, 122245.
17 P. S. Kharkar, G. Soni, V. Rathod, S. Shetty, M. Gupta and K. S. Yadav, *Drug Dev. Res.*, 2020, **81**, 823–836.
18 C. Klein, U. Brinkmann, J. M. Reichert and R. E. Kontermann, *Nat. Rev. Drug Discovery*, 2024, **23**, 301–319.
19 S. Khajeh, M. R. Tohidkia, A. Aghanejad, T. Mehdipour, F. Fathi and Y. Omidi, *Artif. Cells, Nanomed., Biotechnol.*, 2018, **46**, 1082–1090.
20 A. Aghanejad, A. R. Jalilian, Y. Fazaeli, D. Beiki, B. Fateh and A. Khalaj, *J. Radioanal. Nucl. Chem.*, 2014, **299**, 1635–1644.
21 A. Tarighatnia, M. R. Fouladi, M. R. Tohidkia, G. Johal, N. D. Nader, A. Aghanejad and H. Ghadiri, *J. Drug Delivery Sci. Technol.*, 2021, **66**, 102895.
22 N. Hashemzadeh, M. Dolatkhah, K. Adibkia, A. Aghanejad, M. Barzegar-Jalali, Y. Omidi and J. Barar, *Life Sci.*, 2021, **271**, 119110.
23 D. Sun, S. Zhou and W. Gao, *ACS Nano*, 2020, **14**, 12281–12290.
24 S. Raj, S. Khurana, R. Choudhari, K. K. Kesari, M. A. Kamal, N. Garg, J. Ruokolainen, B. C. Das and D. Kumar, *Semin. Cancer Biol.*, 2021, **69**, 166–177.
25 M. Izci, C. Maksoudian, B. B. Manshian and S. J. Soenen, *Chem. Rev.*, 2021, **121**, 1746–1803.
26 T. C. Owens, N. Anton and M. F. Attia, *Acta Biomater.*, 2023, **171**, 19–36.
27 W. Lian and M. Gan, *Biotechnol. Bioprocess Eng.*, 2024, **29**, 185–196.
28 M. Botta, C. F. G. C. Geraldes and L. Tei, *Wiley Interdiscip. Rev.: Nanomed. Nanobiotechnol.*, 2023, **15**, e1858.
29 M. A. Raheem, M. A. Rahim, I. Gul, X. Zhong, C. Xiao, H. Zhang, J. Wei, Q. He, M. Hassan, C. Y. Zhang, D. Yu, V. Pandey, K. Du, R. Wang, S. Han, Y. Han and P. Qin, *OpenNano*, 2023, **12**, 100152.
30 A. L. Frencken, D. Richtsmeier, R. L. Leonard, A. G. Williams, C. E. Johnson, J. A. Johnson, B. Blasiak, A. Orlef, A. Skorupa, M. Sokół, B. Tomanek, W. Beckham, M. Bazalova-Carter and F. C. J. M. van Veggel, *ACS Appl. Mater. Interfaces*, 2024, **16**, 13453–13465.
31 S. Rahmati and A. E. David, *Appl. Mater. Today*, 2024, **37**, 102087.
32 X. Lu, X. Wang, S. Gao, Z. Chen, R. Bai and Y. Wang, *Analyst*, 2023, **148**, 4967–4981.
33 M. Rahman, *NANO*, 2023, **7**, 424–449.
34 X. Tian, W. Li, Q. Quan, Z. Chen, Y. Su, S. Han and Q. Su, *J. Lumin.*, 2024, **269**, 120511.
35 D.-W. Hwang, A. Maekiniemi, R. H. Singer and H. Sato, *Nat. Rev. Genet.*, 2024, **25**, 272–285.
36 H. Liu, R. Wang, H. Gao, L. Chen, X. Li, X. Yu, Y. Wu, Y. Bai, W. Wei and M. Wang, *Adv. Ther.*, 2024, **7**, 2300232.
37 N. Baghban, A. Khoradmehr, A. Afshar, N. Jafari, T. Zendehboudi, P. Rasekh, L. G. Abolfathi, A. Barmak, G. Mohebbi, B. Akmaral, K. A. Askerovich, M. N. Maratovich, H. Azari, M. Assadi, I. Nabipour and A. Tamadon, *Biosensors*, 2023, **13**, 268.
38 H. Hu, *Front. Chem.*, 2020, **8**, 203.

39 J. Pellico, C. M. Ellis and J. J. Davis, *Contrast Media Mol. Imaging*, 2019, 1845637.
40 X. Cao, L. Gu, S. Hu, A. Mukhtar and K. Wu, *Materials*, 2021, **14**, 2238.
41 M. Borges, S. Yu, A. Laromaine, A. Roig, S. Suárez-García, J. Lorenzo, D. Ruiz-Molina and F. Novio, *RSC Adv.*, 2015, **5**, 86779–86783.
42 Y. Luengo Morato, M. Marciello, L. Lozano Chamizo, K. Ovejero Paredes and M. Filice, in *Magnetic Nanoparticle-Based Hybrid Materials*, ed. A. Ehrmann, T. A. Nguyen, M. Ahmadi, A. Farmani and P. Nguyen-Tri, Woodhead Publishing, 2021, pp. 343–386, DOI: **10.1016/B978-0-12-823688-8.00008-9**.
43 P. Wang, W. Sun, J. Guo, K. Zhang, Y. Liu, Q. Jiang, D. Su and X. Sun, *Colloids Surf., B*, 2021, **197**, 111403.
44 A. Banerjee, B. Blasiak, A. Dash, B. Tomanek, F. C. van Veggel and S. Trudel, *Chem. Phys. Rev.*, 2022, **3**, 011304.
45 S. Ponrartana, M. M. Moore, S. S. Chan, T. Victoria, J. R. Dillman and G. B. Chavhan, *Pediatr. Radiol.*, 2021, **51**, 736–747.
46 M. Jeon, M. V. Halbert, Z. R. Stephen and M. Zhang, *Adv. Mater.*, 2021, **33**, 1906539.
47 L. Gu, X. Cao, A. Mukhtar and K. Wu, *J. Biomed. Mater. Res., Part B*, 2021, **109**, 477–485.
48 J.-s. Choi, S. Kim, D. Yoo, T.-H. Shin, H. Kim, M. D. Gomes, S. H. Kim, A. Pines and J. Cheon, *Nat. Mater.*, 2017, **16**, 537–542.
49 J. Dai, Z. Liu, L. Wang, G. Huang, S. Song, C. Chen, T. Wu, X. Xu, C. Hao, Y. Bian, E. A. Rozhkova, Z. Chen and H. Yang, *J. Am. Chem. Soc.*, 2023, **145**, 1108–1117.
50 D. Liu, J. Li, C. Wang, L. An, J. Lin, Q. Tian and S. Yang, *Nanomed.: Nanotechnol., Biol. Med.*, 2021, **32**, 102335.
51 J. Li, J. You, C. Wu, Y. Dai, M. Shi, L. Dong and K. Xu, *Int. J. Nanomed.*, 2018, **13**, 4607.
52 H. Lu, A. Chen, X. Zhang, Z. Wei, R. Cao, Y. Zhu, J. Lu, Z. Wang and L. Tian, *Nat. Commun.*, 2022, **13**, 7948.
53 Z. Wang, X. Xue, H. Lu, Y. He, Z. Lu, Z. Chen, Y. Yuan, N. Tang, C. A. Dreyer, L. Quigley, N. Curro, K. S. Lam, J. H. Walton, T.-y. Lin, A. Y. Louie, D. A. Gilbert, K. Liu, K. W. Ferrara and Y. Li, *Nat. Nanotechnol.*, 2020, **15**, 482–490.
54 S. Mohaghegh, A. Tarighatnia, Y. Omidi, J. Barar, A. Aghanejad and K. Adibkia, *J. Microencapsulation*, 2022, **39**, 394–408.
55 Y. H. Ahn, D. Y. Kang, S.-B. Park, H. H. Kim, H. J. Kim, G.-Y. Park, S.-H. Yoon, Y.-H. Choi, S. Y. Lee and H.-R. Kang, *Radiology*, 2022, **303**, 329–336.
56 C. Do, J. DeAguero, A. Brearley, X. Trejo, T. Howard, G. P. Escobar and B. Wagner, *Kidney360*, 2020, **1**, 561.
57 A. Popov, M. Abakumov, I. Savintseva, A. Ermakov, N. Popova, O. Ivanova, D. Kolmanovich, A. Baranchikov and V. Ivanov, *J. Mater. Chem. B*, 2021, **9**, 6586–6599.
58 M. Patel, A. Atyani, J.-P. Salameh, M. McInnes and S. Chakraborty, *Radiology*, 2020, **297**, 75–83.
59 N. Iyad, M. S. Ahmad, S. G. Alkhatib and M. Hjouj, *Eur. J. Radiol. Open*, 2023, **11**, 100503.
60 A. Uosef, M. Villagran, J. Z. Kubiak, J. Wosik, R. M. Ghobrial and M. Kloc, *Pediatr. Med. Rodz.*, 2020, **16**, 49–52.
61 H. Setiawan, E. Yuba, A. Harada, I. Aoki and K. Kono, *Nano Sel.*, 2021, **2**, 779–790.
62 R. Patil, A. Galstyan, Z. B. Grodzinski, E. S. Shatalova, S. Wagner, L. L. Israel, H. Ding, K. L. Black, J. Y. Ljubimova and E. Holler, *Int. J. Nanomed.*, 2020, **15**, 3057.
63 S. Anbu, S. H. Hoffmann, F. Carniato, L. Kenning, T. W. Price, T. J. Prior, M. Botta, A. F. Martins and G. J. Stasiuk, *Angew. Chem.*, 2021, **133**, 10831–10839.
64 C. Han, T. Xie, K. Wang, S. Jin, K. Li, P. Dou, N. Yu and K. Xu, *J. Nanobiotechnol.*, 2020, **18**, 1–15.
65 D. Du, H.-J. Fu, W.-W. Ren, X.-L. Li and L.-H. Guo, *Biomed. Pharmacother.*, 2020, **121**, 109614.
66 Y. Zhan, S. Shi, E. B. Ehlerding, S. A. Graves, S. Goel, J. W. Engle, J. Liang, J. Tian and W. Cai, *ACS Appl. Mater. Interfaces*, 2017, **9**, 38304–38312.
67 L.-H. Deng, H. Jiang, F.-L. Lu, H.-W. Wang, Y. Pu, C.-Q. Wu, H.-J. Tang, Y. Xu, T.-W. Chen and J. Zhu, *Int. J. Nanomed.*, 2021, **16**, 201.
68 A. Antonelli and M. Magnani, *J. Magn. Magn. Mater.*, 2022, **541**, 168520.
69 S. Fu, Z. Cai and H. Ai, *Adv. Healthcare Mater.*, 2021, **10**, 2001091.
70 D. Bates, S. Abraham, M. Campbell, I. Zehbe and L. Curiel, *PLoS One*, 2014, **9**, e97220.
71 X. Chen, H. Zhou, X. Li, N. Duan, S. Hu, Y. Liu, Y. Yue, L. Song, Y. Zhang and D. Li, *EBioMedicine*, 2018, **30**, 129–137.
72 M. Abdolahi, D. Shahbazi-Gahrouei, S. Laurent, C. Sermeus, F. Firozian, B. J. Allen, S. Boutry and R. N. Muller, *Contrast Media Mol. Imaging*, 2013, **8**, 175–184.
73 X. Cai, Q. Zhu, Y. Zeng, Q. Zeng, X. Chen and Y. Zhan, *Int. J. Nanomed.*, 2019, 8321–8344.
74 M. A. Shevtsov, B. P. Nikolaev, L. Y. Yakovleva, Y. Y. Marchenko, A. V. Dobrodumov, A. L. Mikhrina, M. G. Martynova, O. A. Bystrova, I. V. Yakovenko and A. M. Ischenko, *Int. J. Nanomed.*, 2014, 273–287.
75 N. L. Adolphi, K. S. Butler, D. M. Lovato, T. Tessier, J. E. Trujillo, H. J. Hathaway, D. L. Fegan, T. C. Monson, T. E. Stevens and D. L. Huber, *Contrast Media Mol. Imaging*, 2012, **7**, 308–319.
76 Y.-W. Li, Z.-G. Chen, Z.-S. Zhao, H.-L. Li, J.-C. Wang and Z.-M. Zhang, *World J. Gastroenterol.*, 2015, **21**, 4275.
77 Y. Lu, J. Huang, F. Li, Y. Wang, M. Ding, J. Zhang, H. Yin, R. Zhang and X. Ren, *Magn. Reson. Mater. Phys., Biol. Med.*, 2021, **34**, 581–591.
78 N. Zarghami, M. S. Soto, F. Perez-Balderas, A. A. Khrapitchev, C. S. Karali, V. A. Johanssen, O. Ansorge, J. R. Larkin and N. R. Sibson, *J. Cereb. Blood Flow Metab.*, 2020, **41**, 1592–1607.
79 Z. Salehnia, D. Shahbazi-Gahrouei, A. Akbarzadeh, B. Baradaran, S. Farajnia and M. Naghibi, *IET Nanobiotechnol.*, 2019, **13**, 400–406.
80 R. Malekzadeh, B. Babaye Abdollahi, M. Ghorbani, J. Pirayesh Islamian and T. Mortezazadeh, *Int. J. Polym. Mater. Polym. Biomater.*, 2022, 1–12.

81 X. Li, S. Xia, W. Zhou, R. Ji and W. Zhan, *Int. J. Nanomed.*, 2019, **14**, 2397.
82 C. F. Geraldes, *Molecules*, 2024, **29**, 1352.
83 S. Suárez-García, N. Arias-Ramos, C. Frias, A. P. Candiota, C. Arús, J. Lorenzo, D. Ruiz-Molina and F. Novio, *ACS Appl. Mater. Interfaces*, 2018, **10**, 38819–38832.
84 M. J. Jacobin-Valat, K. Deramchia, S. Mornet, C. E. Hagemeyer, S. Bonetto, R. Robert, M. Biran, P. Massot, S. Miraux and S. Sanchez, *NMR Biomed.*, 2011, **24**, 413–424.
85 J. Greffier, N. Villani, D. Defez, D. Dabli and S. Si-Mohamed, *Diagn. Interv. Imaging*, 2023, **104**, 167–177.
86 A. Galluzzo, G. Danti, E. Bicci, M. Mastrorosato, E. Bertelli and V. Miele, *Semin. Ultrasound CT MRI*, 2023, **44**, 136–144.
87 L. M. Nieves, J. C. Hsu, K. C. Lau, A. D. Maidment and D. P. Cormode, *Nanoscale*, 2021, **13**, 163–174.
88 M. S. Jameel, A. A. Aziz, M. A. Dheyab, B. Mehrdel, P. M. Khaniabadi and B. M. Khaniabadi, *Mater. Today Commun.*, 2021, **27**, 102480.
89 E. Koshevaya, E. Krivoshapkina and P. Krivoshapkin, *J. Mater. Chem. B*, 2021, **9**, 5008–5024.
90 H. Taghavi, M. Bakhshandeh, A. Montazerabadi, H. N. Moghadam, S. B. M. Shahri and M. Keshtkar, *Iran J. Radiol.*, 2020, **17**, e92446.
91 M. Hosseini, Z. Ahmadi, M. Khoobi, S. Dehghani and A. Kefayat, *ACS Sustainable Chem. Eng.*, 2020, **8**, 13085–13099.
92 S. M. Hameed, M. M. Radhi and A. A. Mohsin, *J. Nanostruct.*, 2021, **11**, 543–553.
93 D. Luo, X. Wang, C. Burda and J. P. Basilion, *Cancers*, 2021, **13**, 1825.
94 M. A. Kimm, M. Shevtsov, C. Werner, W. Sievert, W. Zhiyuan, O. Schoppe, B. H. Menze, E. J. Rummeny, R. Proksa and O. Bystrova, *Cancers*, 2020, **12**, 1331.
95 T. Nakagawa, K. Gonda, T. Kamei, L. Cong, Y. Hamada, N. Kitamura, H. Tada, T. Ishida, T. Aimiya, N. Furusawa, Y. Nakano and N. Ohuchi, *Sci. Technol. Adv. Mater.*, 2016, **17**, 387–397.
96 M. F. Ghaziyani, M. P. Moghaddam, D. Shahbazi-Gahrouei, M. Ghavami, A. Mohammadi, M. M. Abbasi and B. Baradaran, *Adv. Pharm. Bull.*, 2018, **8**, 599.
97 M. Zenze, A. Daniels and M. Singh, *Pharmaceutics*, 2023, **15**, 398.
98 J. S. Chen, J. Chen, S. Bhattacharjee, Z. Cao, H. Wang, S. D. Swanson, H. Zong, J. R. Baker and S. H. Wang, *J. Nanobiotechnol.*, 2020, **18**, 1–9.
99 J. R. Ashton, E. B. Gottlin, E. F. Patz Jr, J. L. West and C. T. Badea, *PLoS One*, 2018, **13**, e0206950.
100 D. M. Griffith, H. Li, M. V. Werrett, P. C. Andrews and H. Sun, *Chem. Soc. Rev.*, 2021, **50**, 12037–12069.
101 H. Zhao, J. Wang, X. Li, Y. Li, C. Li, X. Wang, J. Wang, S. Guan, Y. Xu and G. Deng, *J. Colloid Interface Sci.*, 2021, **604**, 80–90.
102 L. Li, Y. Lu, C. Jiang, Y. Zhu, X. Yang, X. Hu, Z. Lin, Y. Zhang, M. Peng and H. Xia, *Adv. Funct. Mater.*, 2018, **28**, 1704623.
103 M. Oumano, L. Russell, M. Salehjahromi, L. Shanshan, N. Sinha, W. Ngwa and H. Yu, *J. Appl. Clin. Med. Phys.*, 2021, **22**, 337–342.
104 H. Su, Y. Liao, F. Wu, X. Sun, H. Liu, K. Wang and X. Zhu, *Colloids Surf., B*, 2018, **170**, 194–200.
105 Y. Zhang, Z. Yang, L. Song, Y. Li and Q. Lin, *J. Colloid Interface Sci.*, 2024, **659**, 1003–1014.
106 A. Tarighatnia, G. Johal, A. Aghanejad, H. Ghadiri and N. Nader, *Front. Biomed. Technol.*, 2021, **8**, 226–235.
107 J. Wang, L. Li, Y. Li, L. Liu, J. Li, X. Li, Y. Zhu, X. Zhang and H. Lu, *Nanomed.: Nanotechnol., Biol. Med.*, 2023, **47**, 102617.
108 J. S. Chen, J. Chen, S. Bhattacharjee, Z. Cao, H. Wang, S. D. Swanson, H. Zong, J. R. Baker and S. H. Wang, *J. Nanobiotechnol.*, 2020, **18**, 1–9.
109 D. Hara, W. Tao, T. M. Totiger, A. Pourmand, N. Dogan, J. C. Ford, J. Shi and A. Pollack, *Int. J. Radiat. Oncol., Biol., Phys.*, 2021, **111**, 220–232.
110 G. Sharma, A. Kumar, S. Sharma, M. Naushad, R. P. Dwivedi, Z. A. Alothman and G. T. Mola, *J. King Saud Univ., Sci.*, 2019, **31**, 257–269.
111 A. K. Gupta and M. Gupta, *Biomaterials*, 2005, **26**, 3995–4021.
112 S. Zhang, Y. Qi, H. Yang, M. Gong, D. Zhang and L. Zou, *J. Nanopart. Res.*, 2013, **15**, 1–9.
113 D. S. Idris and A. Roy, *Crystals*, 2023, **13**, 637.
114 H. Makada, S. Habib and M. Singh, *Sci. Afr.*, 2023, **20**, e01700.
115 F. Cavagna, C. Luchinat, A. Scozzafava and Z. Xia, *Magn. Reson. Med.*, 1994, **31**, 58–60.
116 H. Aviv, S. Bartling, I. Grinberg and S. Margel, *J. Biomed. Mater. Res., Part B*, 2013, **101**, 131–138.
117 F. He, H. Ji, L. Feng, Z. Wang, Q. Sun, C. Zhong, D. Yang, S. Gai, P. Yang and J. Lin, *Biomaterials*, 2021, **264**, 120453.
118 E. Kozma and P. Kele, *Top. Curr. Chem.*, 2024, **382**, 7.
119 N. Ma, Y. Liu, D. Chen, C. Wu and Z. Meng, *Biomacromolecules*, 2022, **23**, 4825–4833.
120 M. Arruebo, M. Valladares and Á. González-Fernández, *J. Nanomater.*, 2009, **2009**, 439389.
121 O. V. Zakharova, I. A. Vasyukova and A. A. Gusev, *Nanobiotechnol. Rep.*, 2023, **18**, 165–188.
122 A. Vaidya, A. Shankardass, M. Buford, R. Hall, P. Qiao, H. Wang, S. Gao, J. Huang, M. F. Tweedle and Z.-R. Lu, *Chem. Biomed. Imaging*, 2024, DOI: **10.1021/cbmi.4c00002**.
123 J. C. Hsu, Z. Tang, O. E. Eremina, A. M. Sofias, T. Lammers, J. F. Lovell, C. Zavaleta, W. Cai and D. P. Cormode, *Nat. Rev. Methods Primers*, 2023, **3**, 30.
124 K. Zhou, Z.-Z. Li, Z.-M. Cai, N.-N. Zhong, L.-M. Cao, F.-Y. Huo, B. Liu, Q.-J. Wu and L.-L. Bu, *Pharmacol. Res.*, 2023, **198**, 106989.